ACS SENSORS

pubs.acs.org/acssensors

Article

Visual Analysis and Inhibitor Screening of Leucine Aminopeptidase, a Key Virulence Factor for Pathogenic Bacteria-Associated Infection

Ming Zhang,[▽] Zhenhao Tian,[▽] Jiayue Wang,[▽] Xiangge Tian, Chao Wang,* Jingnan Cui, Xiaokui Huo, Lei Feng,* Zhenlong Yu, and Xiaochi Ma*

Cite This: https://doi.org/10.1021/acssensors.1c01161

Read Online

ACCESS | Metrics & More | Article Recommendations | Supporting Information

ABSTRACT: Leucine aminopeptidase (LAP) is a hydrolase for the hydrolysis of peptides or proteins containing a leucine residue at the N-terminal. It is also known to be a key virulence factor for the pathogenic abilities of various pathogens causing infectious diseases, which indicated a new insight into the diagnosis and therapy of pathogenic infections. A new fluorescent probe (*S*)-2-amino-*N*-(4-(((6,8-dichloro-9,9-dimethyl-7-oxo-7,9-dihydroacridin-2-yl)oxy)-methyl)phenyl)-4-methylpentanamide (DDBL) containing DDAO as the fluorophore and leucine as the recognition group was developed for LAP. By real-time visual sensing of LAP, six bacteria with LAP expression were identified efficiently from human feces, as well as by sensitive visual analysis using native-PAGE specially stained with DDBL. Furthermore, a high throughput screening system established with DDBL was applied to identify a natural inhibitor (3-acetyl-11-keto-β-boswellic acid, AKBA), which could attenuate mouse sepsis induced by *Staphylococcus aureus*. Therefore, the visual sensing of LAP by DDBL suggested the application for target bacteria identification and LAP homolog analysis as well as potential inhibitor expounding for treatment of bacterial infections.

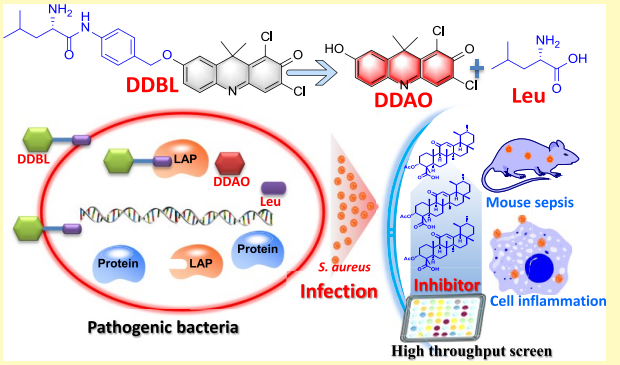

KEYWORDS: *leucine aminopeptidase, fluorescent biosensor, bacteria, sepsis, inhibitor*

Leucine aminopeptidase (LAP EC 3.4.11.1), known as an important exopeptidase, specially hydrolyzes the leucine residue from the N-terminal of proteins or peptides.[1] Widely existing in different organisms, LAP is revealed to participate in various biological, physiological, and pathological processes.[2−4] In contrast to the expression in cancer cells or tissues of mammals, high homology LAPs were obtained from Gram-negative or -positive bacteria as well as functional gene sequencing,[5−14] such as *Escherichia coli*, *Aeromonas proteolytica*, *Streptomyces lividans*, *Pseudomonas aeruginosa*, *Bacillus sp.* N2, and marine *Pseudomonas*. As now bacterial LAP as an important virulence factor has been found the association with the formation of bacterial biofilm and the pathogenicity of pathogens, which induce acute or chronic diseases.[15−18]

Among the various pathogenic bacteria, *S. aureus* is a strongly virulent pathogen capable of causing plenty of infectious diseases in hospitals and communities, leading to more fatalities than HIV/AIDS. More importantly, the continued emergence of highly pathogenic methicillin-resistant *S. aureus* bacteria is becoming a major public health concern in the world.[19,20] LAP located in the cytosol was identified to be the key virulence factor, is required for the survival of *S. aureus* inside human macrophages, and strongly affected the pathogenic abilities of *S. aureus*.[21] Above all, LAP as the key virulence factor of pathogenic bacteria gave a new insight for the diagnosis and treatment of infectious diseases caused by pathogens. Thus, a sensitive and selective analysis method for visually tracing and identifying bacterial LAP and even screening potential inhibitors is highly in demand.

For the activity assay of biological enzymes, fluorescent probes are recently developed powerful tools for the visual detection of functional proteins, with characteristics of ultrasensitivity, high spatiotemporal resolution, and simplicity in operation.[22−30] Until now, various fluorescent probes have been developed for monitoring LAP in mammalian living samples, such as living cells, tumor tissues, a xenograft tumor mice model, and a zebrafish model.[31−41] However, no biosensor was developed for bacterial LAP analysis and detection and even for the application for antibacterials.

In our study, a new fluorescent probe (*S*)-2-amino-*N*-(4-(((6,8-dichloro-9,9-dimethyl-7-oxo-7,9-dihydroacridin-2-yl)-oxy)methyl)phenyl)-4-methylpentanamide (DDBL) is developed for the visual detection of bacterial LAP, which is

Received: June 4, 2021
Accepted: August 11, 2021

composed of a near-infrared (NIR) fluorophore 7-hydroxy-9*H*-(1,3-dichloro-9,9-dimethylacridin-2-one) (DDAO) as the reporter and L-leucine as the triggered moieties. Using DDBL, the activity of LAP was assayed sensitively, and the identification of the bacteria from fecal samples and discovery of potential inhibitors by a high-throughput screening technique were performed, displaying the potential application for the treatment of *S. aureus* infection.

RESULTS AND DISCUSSION

DDBL as a NIR Fluorescent Probe for LAP. LAP is known for its protease activity, removing the L-leucine moiety from the N-terminal of various peptides and proteins by the hydrolysis of amide bonds. By simulating the biochemical reaction, a fluorescent molecule was developed as the special biosensor of LAP, which was composed of a NIR fluorophore DDAO and leucine linked by*p*-aminophenethyl alcohol. Using L-leucine moieties as the recognition group, DDBL can be hydrolyzed by LAP, yielding DDAO as the fluorophore (Figure 1a). The distinct absorbance spectra of DDBL and DDAO

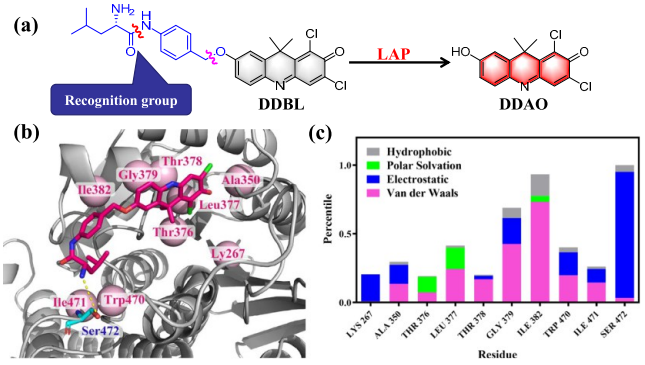

Figure 1. (a) Illustration of the enzymatic hydrolysis of DDBL mediated by LAP. (b) Interaction format of DDBL bounded in LAP. (c) Important roles of key residues in the interaction between DDBL and LAP.

displayed a large red shift, and a strong fluorescence intensity was observed for DDAO at 660 nm, compared to the absence of fluorescence of DDBL (Figure S1). In addition, HPLC has been applied to detect DDAO in the enzymatic solution containing DDBL and LAP, which confirmed the yield of DDAO (Figure S2). *In silico* docking has been performed to simulate the interactions between DDBL and LAP (Figure 1b), which revealed the existence of non-polar interactions (purple spheres) and hydrogen bonds (cyan sticks, yellow line). On the basis of detailed energy decomposition, key residues playing important roles in the interaction format for DDBL bounded in LAP also have been indicated, as shown in Figure 1c. Thus, DDBL shows promise as a suitable substrate of LAP as well as an excellent NIR fluorescent biosensor.

Fluorescence Behavior of DDBL toward LAP. The hydrolysis of DDBL by LAP in a series concentration was carried out, resulting in sequential fluorescence curves that correlated with LAP concentrations (Figure 2c). Furthermore, a good linear relationship was observed between the fluorescence intensities (λ_{em} of 660 nm) and LAP concentrations, indicating the application for quantitative LAP activity assay with a limit of detection (LOD) of 0.0002 U/mL (3σ/k) (Figure 2b). In addition, the substrate specificity of DDBL toward LAP was investigated in the presence of different

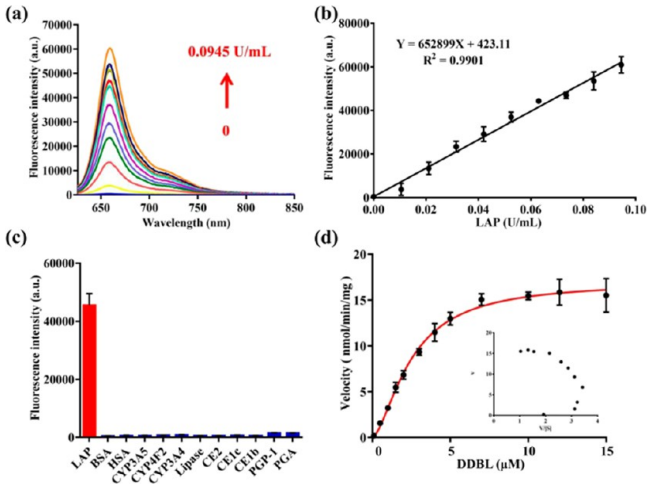

Figure 2. (a) Fluorescence response of DDBL toward LAP with different concentrations. (b) Linear relationship between fluorescence intensity and LAP concentrations. (c) Fluorescence response of DDBL toward various functional enzymes. (d) Kinetics of the hydrolysis of DDBL mediated by LAP.

biological enzymes. As shown in Figure 2c, DDBL could be hydrolyzed by LAP selectively. In addition, the kinetics has been characterized as the Hill kinetics model, with K_m = 2.485 ± 0.3 μM and V_{max} = 17.01 ± 0.05 nmol/min/mg (Figure 2d). Furthermore, interferences about various factors (amino acids, ions, pH value, temperature, etc.) on the fluorescence intensity of DDBL and the enzymatic hydrolysis in the presence of LAP have been evaluated (Figures S4−S7). Above all, DDBL has been developed to be a fluorescent biosensor of LAP by full validation.

Identification of Intestinal Bacteria with LAP Expression. It is well known that intestinal microbiota plays important roles in the health and disease of hosts. LAP secreted by intestinal bacteria participates in the metabolism of exogenous/endogenous peptides or proteins and is involved in the metabolic process of bacteria or hosts. In addition, LAP is associated with the pathogenicity of intestinal bacteria, inducing infections in the digestive organs and lung and even bacteremia. Thus, using the developed fluorescent molecule, the expression of LAP in intestinal bacteria is expected to be explored in our study.

Fresh stool samples from healthy humans were applied for cultivation of intestinal bacteria. When the bacterial colonies were observed on agar plates, DDBL was dropped for a co-incubation and detection of endogenous LAP. Under a fluorescence imager, colonies with strong fluorescence signals indicated expression of active LAP, which were picked for purification (Figure 3a). In combination with 18*S* rRNA gene sequencing, six target bacteria strains were identified as *Enterobacter hormaechei* subsp (1), *Escherichia fergusonii* ATCC 35469 (2), *Shigella flexneri* strain ATCC 29903 (3), *Klebsiella variicola* strain F2R9 (4), *Raoultella planticola* strain NBRC 14939 (5), and *Pluralibacter gergoviae* ATCC 33028 (6) (Figure 3b). The hydrolysis of DDBL along with the production of DDAO mediated by LAP in the *K. variicola* bacteria strain F2R9 was detected using HPLC (Figure S8). In addition, the expressions of LAP in these cultivated bacterial strains were also confirmed by RT-PCR (Figure 3c). Obviously, under the guidance of visual sensing of endogenous

https://doi.org/10.1021/acssensors.1c01161
ACS Sens. XXXX, XXX, XXX−XXX

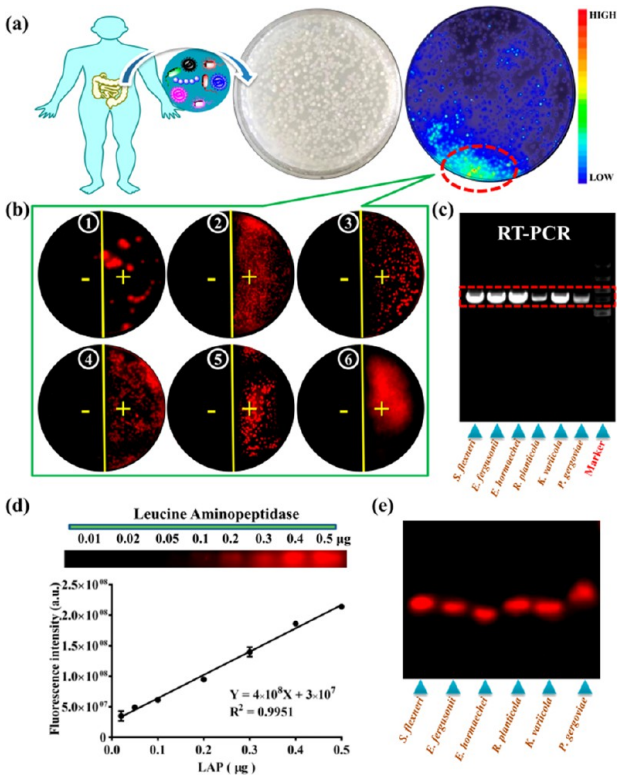

Figure 3. Visual sensing of endogenous LAP in bacteria. (a) Cultivation and identification of intestinal bacteria with active LAP. (b) Fluorescence imaging of six isolated intestinal bacteria, i.e., *E. hormaechei* subsp. (1), *E. fergusonii* ATCC 35469 (2), *S. flexneri* strain ATCC 29903 (3), *K. variicola* strain F2R9 (4), *R. planticola* strain NBRC 14939 (5), and *P. gergoviae* ATCC 33028 (6). (c) RT-PCR for LAP expression in the six isolated bacteria strains. (d) Visual analysis of recombined LAP on native-PAGE stained by DDBL. (e) Visual analysis of active LAP from lysates of the six bacteria on native-PAGE stained by DDBL.

LAP by DDBL, target bacteria with active LAP can be identified successfully from human feces.

To obtain a more intuitive analysis of active LAP, a native-PAGE stained by DDBL was developed. As shown in Figure 3d, a series of active recombined LAP at different concentrations were analyzed on native-PAGE, which displayed fluorescence bands stained by DDBL. A good linear relationship was observed between the fluorescence intensity and LAP concentrations of these fluorescence bands. However, no band showed on the gel stained with silver or Coomassie blue (Figure S9). Therefore, stained with DDBL, the native-PAGE was used as a sensitive and selective analysis technique for active LAP. Additionally, lysates of the six isolated intestinal bacteria were analyzed by the developed native-PAGE using DDBL as the special sensor (Figure 3e and Figure S10). It was obvious that similar fluorescence bands were displayed corresponding to the individual bacterial lysate. Similar electrophoretic distances indicated the high homology of these LAPs, which were also confirmed by amino acid sequence comparison (Figure S11). Above all, using DDBL as the sensitive special stain, active LAP from functional bacteria can be visually analyzed on the native-PAGE.

Preparation of LAP Inhibitors Using High-Throughput Screening System Established by DDBL. LAP as the key virulence factor of pathogenic bacteria was suggested as a novel target for the prevention and treatment of bacterial infection. Potential inhibitors of LAP showed promise in the clinical usage for pathogenic bacteria-associated disease. In our study, on the basis of the fluorescent biosensor, a high-throughput screening system for the activity of LAP has been established, which was applied for the inhibitor screening. A total of 54 herb medicines have been evaluated for their inhibitory effects against LAP, indicating the significant inhibitory effects of olibanum (8) and *R. officinalis* (54) (Figure 4b and Figure S12). Then, the major active

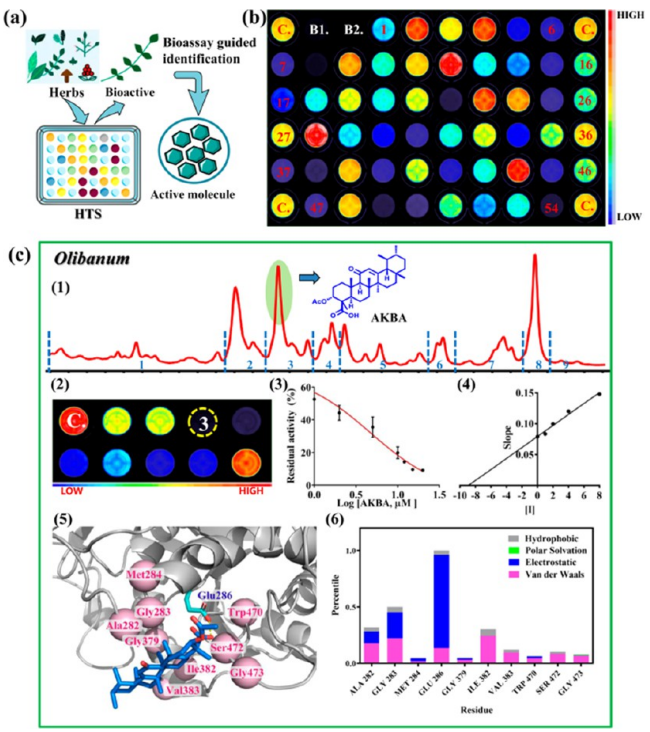

Figure 4. Preparation of LAP inhibitors from olibanum. (a) Illustration for inhibitor identification using the high-throughput screening system. (b) Inhibitory effects of 54 herb medicines on LAP. (c) Identification of LAP inhibitors from olibanum. (1) HPLC chromatogram of olibanum and preparative fractions. (2) Inhibitory effects of fractions on LAP. (3) Inhibitory activity of AKBA on LAP. (4) Inhibitory kinetics of AKBA on LAP. (5) Overview of the simulated interactions between AKBA and LAP. (6) Key residues and major interactions.

constituents were designed to be identified from olibanum and *R. officinalis*, respectively. The extract of olibanum was separated into nine fractions by preparative HPLC, which were evaluated for their inhibitory effects on LAP (Figure 4c). For fraction 3 with the strongest inhibitory activity, the chemical constituent was determined to be 3-acetyl-11-keto-β-boswellic acid (AKBA) as a triterpenoid by further purification and spectroscopic data. AKBA inhibited the hydrolase activity of LAP significantly (IC_{50} of 1.38 ± 0.27 μM), displaying mixed inhibition kinetics (K_i 2.44 ± 0.11 μM) (Figure S13). The inhibitory mechanism was investigated by the simulated interactions between AKBA and LAP, which showed mostly non-polar interactions (purple spheres). A stable hydrogen bond formed between AKBA and the Glu286 residue (Figure 4c).

Similarly, two diterpenoids carnosol and carnosic acids were identified as LAP inhibitors from the chromatographic fractions 7 and 8 of *R. officinalis*, respectively (Figure S14).

https://doi.org/10.1021/acssensors.1c01161
ACS Sens. XXXX, XXX, XXX−XXX

Both natural compounds could inhibit the hydrolase activity of LAP moderately, with an IC_{50} of 5.98 ± 0.2 and 15.52 ± 2.59 μM. Furthermore, interactions between two inhibitors and LAP were also simulated, exhibiting the key residues to be ASP 349 and GLU286 toward carnosol and carnosic acids, respectively.

Inhibitory Effects of the Screened Inhibitors Against the Pathogenicity of *S. aureus*. *S. aureus* is a virulent pathogen capable of causing plenty of infectious diseases, with LAP as the key virulence factor. Using DDBL as the fluorescent probe, *S. aureus* LAP was sensed and a strong fluorescence signal was observed for *S. aureus* under a confocal laser scanning microscope (Figure 5). On the other hand, a weak fluorescence signal was displayed by *S. aureus* with co-incubation of DDBL and LAP inhibitors AKBA and carnosic acid. Thus, active endogenous LAP was confirmed for *S. aureus*, together with special sensing of LAP by DDBL and potential inhibitory effects of AKBA and carnosic acid.

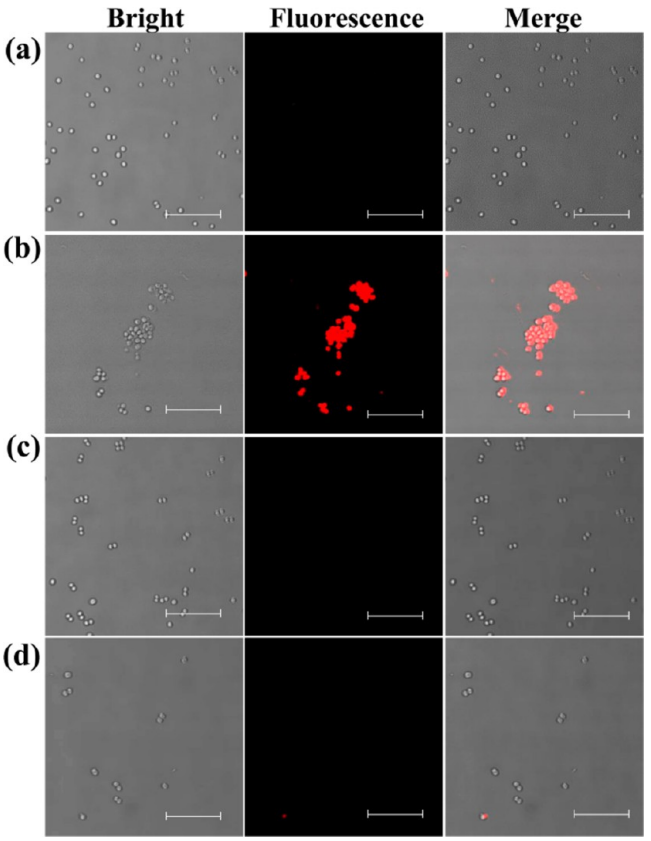

Figure 5. Fluorescence imaging of *S. aureus* by sensing of endogenous LAP using DDBL. (a) Blank group. (b) *S. aureus* co-incubated with DDBL. (c) *S. aureus* co-incubated with DDBL in the presence of AKBA. (d) *S. aureus* co-incubated with DDBL in the presence of carnosic acid. (Scale bars are 10 μm. λ_{ex} = 633 nm and λ_{em} = 645−690 nm).

AKBA and carnosic acid (CAA) as the screened LAP inhibitors showed promising inhibitory effects against the pathogenicity of *S. aureus* and attenuating effects against infection of mice induced by *S. aureus*. In the present work, *S. aureus* was applied to infect RAW 264.7 murine macrophage cells. AKBA (25 μM) and CAA (50 μM) were used to inhibit endogenous LAP in the infection process at a concentration where there is no interference in the proliferation of *S. aureus* (Figures S16 and S17). After the infection by *S. aureus*, the loading amount of *S. aureus* and inflammatory cytokines interleukin-6 (IL-6) and tumor necrosis factor-alpha (TNF-α) in RAW 264.7 cells were evaluated. As shown in Figure 6a, fewer *S. aureus* were cultured from the AKBA-treated group, along with fewer IL-6 and TNF-α, indicating the significant inhibitory effects of AKBA against the pathogenicity of *S. aureus* for the infection of RAW264.7 cells. Similarly, CAA also displayed interference in RAW264.7 infection by *S. aureus*, which is weaker than AKBA.

In addition, mouse sepsis induced by *S. aureus* has been used to evaluate the attenuating effects of AKBA. After pre-incubation by AKBA, *S. aureus* was applied to infect mice by intraperitoneal injection. In view of this, sepsis symptoms have been observed for the model group infected with untreated *S. aureus* in comparison with the vehicle group. The attenuating effects of AKBA have been evaluated completely. After the infection, death has been observed in different groups within 24 h, and the survival rates were determined as 100% (Veh.), 91.7% (AKBA), and 41.7% (model). As shown in Figure 7a, sepsis mice were listless with disordered hair compared with the vehicle group. However, mice infected with AKBA-treated *S. aureus* displayed a better healthy state. The survival mice were evaluated for their sepsis by loaded bacteria count, inflammatory cytokines, and histology. First, a lower bacteria count was determined for various organs and tissues (heart, lung, liver, kidney, spleen, kidney, belly, and blood) from mice of the AKBA group in comparison with the model group (Figure 7b). Additionally, blood culture agar plates with bacterial colonies were stained with DDBL displaying strong fluorescence intensity, which was convenient for bacteria counting (Figure 7c). It was obvious that fewer fluorescence bacteria colonies existed on the agar plate of the AKBA group. Then, a weaker inflammatory response was observed for mice infected with AKBA-treated *S. aureus* on the basis of IL-6, TNF-α, and IFN-γ assays in the plasma, heart, lung, and liver (Figure 7d−g). Furthermore, distinct histology of the mice heart, lung, liver, and kidney was also observed between the AKBA group and model group. Therefore, *S. aureus* treated with AKBA displayed weak pathogenicity for infectious diseases (sepsis, etc.). AKBA and even the natural medicine olibanum as the inhibitor of LAP showed a new insight into the therapy of bacterial infectious diseases.

CONCLUSIONS

LAP is a key virulence factor of the pathogenicity of bacteria causing various infectious diseases. The real-time analysis of bacterial LAP together with inhibitor development is in demand for the diagnosis and therapy of bacterial infections. Using a NIR fluorophore DDAO, a new fluorescent probe DDBL was developed for visual real-time sensing of LAP. Intestinal bacteria possessing active LAP can be specially identified from a mix sample, and individual LAP can be visually analyzed on native-PAGE based on the visual sensing of LAP by DDBL. In addition, a high-throughput screening system was established by DDBL for the inhibitor screening. As a result, natural inhibitors were prepared efficiently, among which AKBA as a potential LAP inhibitor could attenuate mouse sepsis induced by *S. aureus*.

https://doi.org/10.1021/acssensors.1c01161
ACS Sens. XXXX, XXX, XXX−XXX

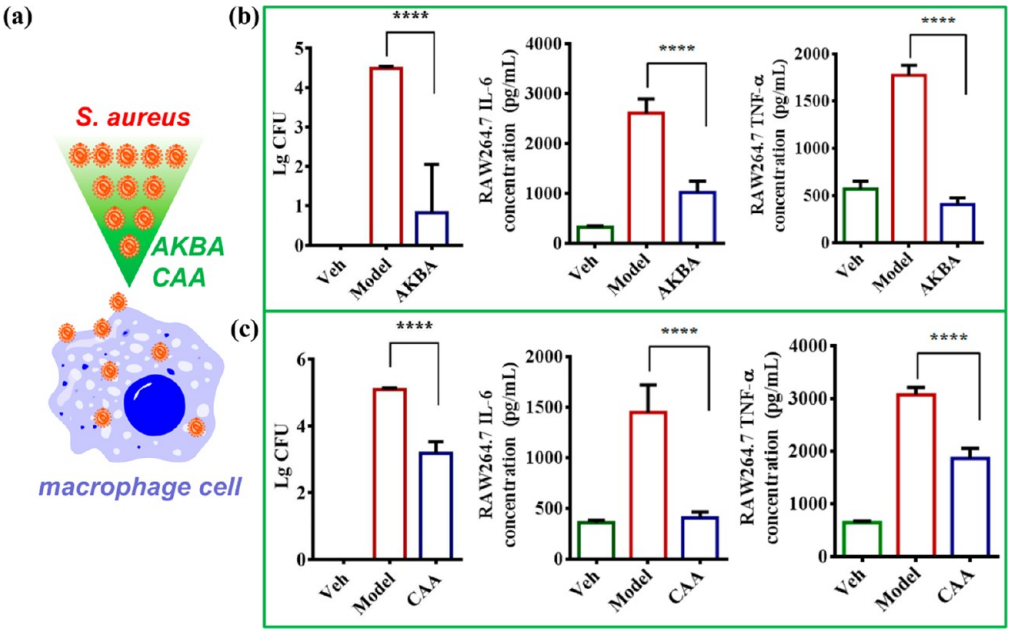

Figure 6. Infection of murine RAW 264.7. Interference of LAP inhibitors on RAW 264.7 macrophage cell infection by *S. aureus*. (a) Illustration for the infection. Antibacterial effects of AKBA (b) and CAA (c). Each bar represents mean ± SD. Student's *t* test, ****$P < 0.0001$, compared with those of *S. aureus*-treated cells.

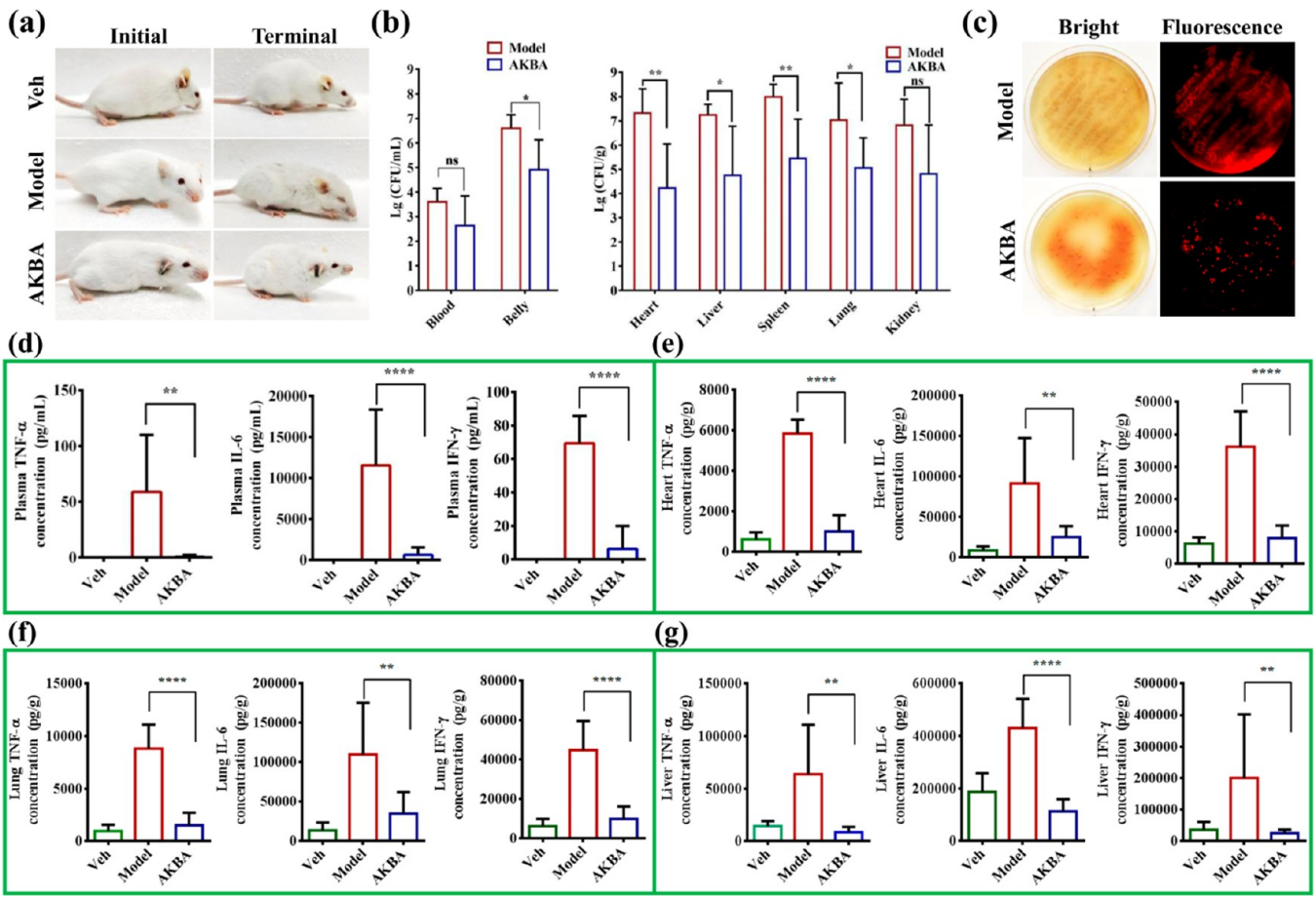

Figure 7. Attenuating effects of AKBA against mouse sepsis induced by *S. aureus*. (a) Phenotype of mice. (b) Bacterial infection of various organs from experimental mice. (c) Images of blood culture agar plates stained with DDBL. Inflammatory evaluation of plasma (d), heart (e), lung (f), and liver (g). Veh. $n = 6$, model $n = 5$, and AKBA $n = 7$. Each bar represents mean ± SD. Student's *t* test, **$P < 0.01$ and ****$P < 0.0001$, compared with those of *S. aureus*-treated mice.

https://doi.org/10.1021/acssensors.1c01161
ACS Sens. XXXX, XXX, XXX−XXX

■ ASSOCIATED CONTENT

Supporting Information

The Supporting Information is available free of charge at https://pubs.acs.org/doi/10.1021/acssensors.1c01161.

Apparatus and methods, synthesis and characterization of compounds, spectroscopy, fluorescence behavior of DDBL, identification of inhibitors, inhibition kinetics, and bioimaging data (PDF)

■ AUTHOR INFORMATION

Corresponding Authors

Chao Wang − *Dalian Key Laboratory of Metabolic Target Characterization and Traditional Chinese Medicine Intervention, College of Integrative Medicine, College of Pharmacy, Dalian 116044, China;* orcid.org/0000-0002-6251-7908; Email: wach_edu@sina.com

Lei Feng − *Dalian Key Laboratory of Metabolic Target Characterization and Traditional Chinese Medicine Intervention, College of Integrative Medicine, College of Pharmacy, Dalian 116044, China; School of Chemistry and Chemical Engineering, Henan Normal University, Xinxiang 453007, China;* orcid.org/0000-0003-2377-0190; Email: leifeng@dmu.edu.cn

Xiaochi Ma − *Dalian Key Laboratory of Metabolic Target Characterization and Traditional Chinese Medicine Intervention, College of Integrative Medicine, College of Pharmacy, Dalian 116044, China; Jiangsu Key Laboratory of New Drug Research and Clinical Pharmacy, Xuzhou Medical University, Xuzhou 221004, China;* orcid.org/0000-0003-4397-537X; Email: maxc1978@163.com

Authors

Ming Zhang − *Dalian Key Laboratory of Metabolic Target Characterization and Traditional Chinese Medicine Intervention, College of Integrative Medicine, College of Pharmacy, Dalian 116044, China; State Key Laboratory of Fine Chemicals, Dalian University of Technology, Dalian 116024, China*

Zhenhao Tian − *School of Life Sciences, Northwestern Polytechnical University, Xi'an 710072, China*

Jiayue Wang − *Dalian Key Laboratory of Metabolic Target Characterization and Traditional Chinese Medicine Intervention, College of Integrative Medicine, College of Pharmacy, Dalian 116044, China; Department of Pharmacy, Peking University Shenzhen Hospital, Shenzhen 518036, China;* orcid.org/0000-0001-5068-631X

Xiangge Tian − *Dalian Key Laboratory of Metabolic Target Characterization and Traditional Chinese Medicine Intervention, College of Integrative Medicine, College of Pharmacy, Dalian 116044, China*

Jingnan Cui − *State Key Laboratory of Fine Chemicals, Dalian University of Technology, Dalian 116024, China;* orcid.org/0000-0002-6104-5056

Xiaokui Huo − *Dalian Key Laboratory of Metabolic Target Characterization and Traditional Chinese Medicine Intervention, College of Integrative Medicine, College of Pharmacy, Dalian 116044, China*

Zhenlong Yu − *Dalian Key Laboratory of Metabolic Target Characterization and Traditional Chinese Medicine Intervention, College of Integrative Medicine, College of Pharmacy, Dalian 116044, China*

Complete contact information is available at: https://pubs.acs.org/10.1021/acssensors.1c01161

Author Contributions

[▽]M.Z., Z.T., and J.W. contributed equally to this work.

Notes

The authors declare no competing financial interest.

■ ACKNOWLEDGMENTS

This work was supported financially by the National Natural Science Foundation of China (nos. 81930112 and 81872970), the National Key R&D Program of China (2018YFC1705900), the Dalian Science and Technology Leading Talents Project (2019RD15), the Liaoning Provincial Natural Science Foundation (20180550761 and 2019-BS-056), the Liaoning Revitalization Talents Program (XLYC1907017), and the Open Research Fund of the School of Chemistry and Chemical Engineering, Henan Normal University for support (2021YB07).

■ REFERENCES

(1) Drinkwater, N.; Malcolm, T. R.; McGowan, S. M17 aminopeptidases diversify function by moderating their macromolecular assemblies and active site environment. *Biochimie* **2019**, *166*, 38−51.

(2) Wu, M.; Yan, M.; Xu, J.; Liang, Y.; Gu, X.; Xie, Y.; Jing, B.; Lai, W.; Peng, X.; Yang, G. Expression, tissue localization and serodiagnostic potential of *Echinococcus granulosus* leucine aminopeptidase. *Int. J. Mol. Sci.* **2018**, *19*, 1063.

(3) Timm, J.; Valente, M.; García-Caballero, D.; Wilson, K. S.; González-Pacanowsk, D. Structural characterization of acidic M17 leucine aminopeptidases from the TriTryps and evaluation of their role in nutrient starvation in *Trypanosoma brucei*. *mSphere* **2017**, *2*, e00226−e00217.

(4) Ren, Q.; Fu, S.; Wang, D.; Ju, W.; He, X. Expression, purification and characterization of two leucine aminopeptidases of the blood fluke. *Schistosoma mansoni. Cancer Manag. Res.* **2021**, *13*, 1053−1066.

(5) Vogt, M. V. Purification and properties of an aminopeptidase from *Escherichia coli*. *J. Biol. Chem.* **1970**, *245*, 4760−4769.

(6) Prescott, J. M.; Wilkes, S. H. Aeromonas aminopeptidase. *Method. Enzymol.* **1976**, *45*, 530−543.

(7) Merkel, J. R.; Lee, C. C.; Freund, T. S. A dimeric extracellular, heat-stable aminopeptidase produced by a marine pseudomonad. *BBA-Enzymol.* **1981**, *661*, 32−38.

(8) Qua, D. V.; Shimizu, U.; Taga, N. Purification and some properties of halophilic protease produced by a moderately halophilic marine *Pseudomonas sp. Can. J. Microbiol.* **1981**, *127*, 505−510.

(9) Aphale, J. S.; Strohl, W. R. Purification and properties of an extracellular aminopeptidase from *Streptomyces lividans* 1326. *J. Gen. Microbiol.* **1993**, *139*, 417−424.

(10) Lee, G. D.; Chun, S. S.; Kho, Y. H.; Chun, H. K. Purification and properties of an extracellular leucine aminopeptidase from the Bacillus sp. N2. *J. Appl. Microbiol.* **1998**, *85*, 561−566.

(11) Garcia-Alvarez, N.; Cueva, R.; Suarez-Rendueles, P. Molecular cloning of soluble aminopeptidase from *Saccharomyces cerevisiae*: sequence analysis of aminopeptidase yscII, a putative zinc-metal-lopeptidase. *Eur. J. Biochem.* **1991**, *202*, 993−1002.

(12) Glaser, P.; Kunst, F.; Debarbouille, M.; Vertes, A.; Danchin, A.; Dedonder, R. A gene encoding a tyrosine tRNA synthetase is located near sacS in *Bacillus subtilis. DNA Sequence* **1991**, *1*, 251−261.

(13) Guenet, C.; Lepage, P.; Harris, B. A. Isolation of the leucine aminopeptidase gene from *Aeromonas proteolytica. Evidence for an enzyme precursor. J. Biol. Chem.* **1992**, *267*, 8390−8395.

(14) Sarnovsky, R.; Rea, J.; Makowski, M.; Hertle, R.; Kelly, C.; Antignani, A.; Pastrana, D. V.; Fitzgerald, D. J. Proteolytic cleavage of a C-terminal prosequence, leading to autoprocessing at the N terminus, activates leucine aminopeptidase from *Pseudomonas aeruginosa*. *J. Biol. Chem.* **2009**, *284*, 10243−10253.

(15) Esoda, C. N.; Kuehn, M. J. *Pseudomonas aeruginosa* leucine aminopeptidase influences early biofilm composition and structure via vesicle-associated antibiofilm activity. *MBio* **2019**, *10*, e02548−e02519.
(16) Jarocki, V. M.; Santos, J.; Tacchi, J. L.; Raymond, B. B. A.; Deutscher, A. T.; Jenkins, C.; Padula, M. P.; Djordjevic, S. P. MHJ-0461 is a multifunctional leucine aminopeptidase on the surface of *Mycoplasma hyopneumoniae*. *Open Biol.* **2015**, *5*, 140175.
(17) Peng, C. T.; Liu, L.; Li, C. C.; He, L. H.; Li, T.; Shen, Y. L.; Gao, C.; Wang, N. Y.; Xia, Y.; Zhu, Y. B.; Song, Y. J.; Lei, Q.; Yu, L. T.; Bao, R. Structure-function relationship of aminopeptidase P from *Pseudomonas aeruginosa*. *Front. Microbiol.* **2017**, *8*, 2385.
(18) Correa, A. F.; Bastos, I. M. D.; Neves, D.; Kipnis, A.; Junqueira-Kipnis, A. P.; Santana, J. M. The activity of a hexameric M17 metallo-aminopeptidase is associated with survival of *Mycobacterium tuberculosis*. *Front. Microbiol.* **2017**, *8*, 504.
(19) Carroll, R. K.; Veillard, F.; Gagne, D. T.; Lindenmuth, J. M.; Poreba, M.; Drag, M.; Potempa, J.; Shaw, L. N. The *Staphylococcus aureus* leucine aminopeptidase is localized to the bacterial cytosol and demonstrates a broad substrate range that extends beyond leucine. *Biol. Chem.* **2013**, *394*, 791−803.
(20) Singh, A. K.; Tomar, R. S. D.; Pandya, C. D.; Singh, R. The leucine aminopeptidase of *Staphylococcus aureus* is secreted and contributes to biofilm formation. *Int. J. Infect. Dis.* **2012**, *16*, e375−e381.
(21) Carroll, R. K.; Robison, T. M.; Rivera, F. E.; Davenport, J. E.; Jonsson, I. M.; Florczyk, D.; Tarkowski, A.; Koziel, J. P. J.; Shaw, L. N. Identification of an intracellular M17 family leucine aminopeptidase that is required for virulence in *Staphylococcus aureus*. *Microbes Infect.* **2012**, *14*, 989−999.
(22) Choi, Y.; Shin, S. H.; Jung, H.; Kwon, O.; Seo, J. K.; Kee, J. M. Specific fluorescent probe for protein histidine phosphatase activity. *ACS Sens.* **2019**, *4*, 1055−1062.
(23) Wang, C.; Tian, Z.; Wang, Y.; Zhang, M.; Zhang, B.; Feng, L.; Tian, X.; Huang, H.; Cui, J.; Ma, X. An enzyme-activated NIR fluorescent probe for detecting bacterial glutamyltranspeptidase (γ-GT) and high-throughput screening of its inhibitors. *Sensor. Actuat. B. Chem.* **2021**, *329*, 129225.
(24) Li, L.; Feng, L.; Zhang, M.; He, X.; Luan, S.; Wang, C.; James, T. D.; Zhang, H.; Huang, H.; Ma, X. Visualization of penicillin G acylase in bacteria and high-throughput screening of natural inhibitors using a ratiometric fluorescent probe. *Chem. Commun.* **2020**, *56*, 4640.
(25) Feng, L.; Tian, Z.; Zhang, M.; He, X.; Tian, X.; Yu, Z.; Ma, X.; Wang, C. Real-time identification of gut microbiota with aminopeptidase N using an activable NIR fluorescent probe. *Chin. Chem. Let.* **2021**, DOI: 10.1016/j.cclet.2021.03.056.
(26) Qian, J.; Teng, Z.; Wang, J.; Zhang, L.; Cao, T.; Zheng, L.; Cao, Y.; Qin, W.; Liu, Y.; Guo, H. Visible to near-infrared emission ratiometric fluorescent probe for the detection of Vanin-1 in vivo. *ACS Sens.* **2020**, *5*, 2806−2813.
(27) Li, H. D.; Li, Y. Q.; Yao, Q. C.; Fan, J. L.; Sun, W.; Long, S.; Shao, K.; Du, J. J.; Wang, J. Y.; Peng, X. J. In situ imaging of aminopeptidase N activity in *hepatocellular carcinoma*: a migration model for tumour using an activatable two-photon NIR fluorescent probe. *Chem. Sci.* **2019**, *10*, 1619−1625.
(28) Zhang, H.; Fan, J.; Wang, J.; Zhang, S.; Dou, B.; Peng, X. An Off−On COX-2-Specific Fluorescent Probe: Targeting the Golgi Apparatus of Cancer Cells. *J. Am. Chem. Soc.* **2013**, *135*, 11663−11669.
(29) Tian, Z.; Yan, F.; Tian, X.; Feng, L.; Cui, J.; Deng, S.; Zhang, B.; Xie, T.; Huang, S.; Ma, X. A NIR fluorescent probe for Vanin-1 and its applications in imaging, kidney injury diagnosis, and the development of inhibitor. *Acta. Pharm. Sin. B.* **2021**, DOI: 10.1016/j.apsb.2021.06.004.
(30) Chai, Z.; Shang, J.; Shi, W.; Li, X.; Ma, H. Increase of tyrosinase activity at the wound site in zebrafish imaged by a new fluorescent probe. *Chem. Comm.* **2021**, *57*, 2764−2767.
(31) Chai, Y.; Gao, Y.; Xiong, H.; Lv, W.; Yang, G.; Lu, C.; Nie, J.; Ma, C.; Chen, Z.; Ren, J.; Wang, F. A near-infrared fluorescent probe for monitoring leucine aminopeptidase in living cells. *Analyst* **2019**, *144*, 463−467.
(32) Gu, K.; Liu, Y.; Guo, Z.; Lian, C.; Yan, C.; Shi, P.; Tian, H.; Zhu, W.-H. In situ ratiometric quantitative tracing intracellular leucin aminopeptidase activity via an activatable near-infrared fluorescent probe. *ACS Appl. Mater. Inter.* **2016**, *8*, 26622−26629.
(33) He, X.; Li, L.; Fang, Y.; Shi, W.; Li, X.; Ma, H. In vivo imaging of leucine aminopeptidase activity in drug-induced liver injury and liver cancer via a near-infrared fluorescent probe. *Chem. Sci.* **2017**, *8*, 3479−3483.
(34) Huang, H.; Tanaka, H.; Hammock, B. D.; Morisseau, C. Novel and highly sensitive fluorescent assay for leucine aminopeptidases. *Anal. Biochem.* **2009**, *391*, 11−16.
(35) Huang, S.; Wu, Y.; Zeng, F.; Chen, J.; Wu, S. A turn-on fluorescence probe based on aggregation-induced emission for leucine aminopeptidase in living cells and tumor tissue. *Anal. Chim. Acta* **2018**, *1031*, 169−177.
(36) Huang, Y.; Qi, Y.; Zhan, C.; Zeng, F.; Wu, S. Diagnosing drug-induced liver injury by multispectral optoacoustic tomography and fluorescence imaging using a leucine aminopeptidase-activated probe. *Anal. Chem.* **2019**, *91*, 8085−8092.
(37) Zhou, Z.; Wang, F.; Yang, G.; Lu, C.; Nie, J.; Chen, Z.; Ren, J.; Sun, Q.; Zhao, C.; Zhu, W. H. A ratiometric fluorescent probe for monitoring leucine aminopeptidase in living cells and zebrafish model. *Anal. Chem.* **2017**, *89*, 11576−11582.
(38) Zhang, W.; Liu, F.; Zhang, C.; Luo, J. G.; Luo, J.; Yu, W.; Kong, L. Near-infrared fluorescent probe with remarkable large stokes shift and favorable water solubility for real-time tracking leucine aminopeptidase in living cells and in vivo. *Anal. Chem.* **2017**, *89*, 12319−12326.
(39) Yamamoto, K.; Kamiya, M.; Urano, Y. Highly sensitive fluorescence imaging of cancer with avidin-protease probe conjugate. *Bioorg. Med. Chem. Let.* **2019**, *29*, 126663.
(40) Chen, Y. Fluorescent probes for detection and bioimaging of leucine aminopeptidase. *Mater. Today Chem.* **2020**, *15*, 100216.
(41) Wang, T.; Sun, Q.; Xiong, H.; Ma, C.; Lu, C.; Nie, J.; Yang, G.; Chen, Z.; Zhang, Y.; Ren, J.; Wang, F.; Zhu, W. Rational design of fluorescent probes: improving hydrophilicity, ratiometric and NIR trapping of endogenous leucine aminopeptidase. *Sensor. Actuat. B. Chem.* **2020**, *321*, 128631.

https://doi.org/10.1021/acssensors.1c01161
ACS Sens. XXXX, XXX, XXX−XXX